Published OnlineFirst February 20, 2014; DOI: 10.1158/0008-5472.CAN-13-2876

Cancer Research

Androgen Receptor Splice Variants Determine Taxane Sensitivity in Prostate Cancer

Maria Thadani-Mulero[1], Luigi Portella[1], Shihua Sun[3], Matthew Sung[1], Alexandre Matov[1], Robert L. Vessella[3,4], Eva Corey[3,4], David M. Nanus[1,2], Stephen R. Plymate[5,6], and Paraskevi Giannakakou[1,2]

Abstract

Prostate cancer growth depends on androgen receptor signaling. Androgen ablation therapy induces expression of constitutively active androgen receptor splice variants that drive disease progression. Taxanes are a standard of care therapy in castration-resistant prostate cancer (CRPC); however, mechanisms underlying the clinical activity of taxanes are poorly understood. Recent work suggests that the microtubule network of prostate cells is critical for androgen receptor nuclear translocation and activity. In this study, we used a set of androgen receptor deletion mutants to identify the microtubule-binding domain of the androgen receptor, which encompasses the DNA binding domain plus hinge region. We report that two clinically relevant androgen receptor splice variants, ARv567 and ARv7, differentially associate with microtubules and dynein motor protein, thereby resulting in differential taxane sensitivity *in vitro* and *in vivo*. ARv7, which lacks the hinge region, did not co-sediment with microtubules or coprecipitate with dynein motor protein, unlike ARv567. Mechanistic investigations revealed that the nuclear accumulation and transcriptional activity of ARv7 was unaffected by taxane treatment. In contrast, the microtubule-interacting splice variant ARv567 was sensitive to taxane-induced microtubule stabilization. In ARv567-expressing LuCap86.2 tumor xenografts, docetaxel treatment was highly efficacious, whereas ARv7-expressing LuCap23.1 tumor xenografts displayed docetaxel resistance. Our results suggest that androgen receptor variants that accumulate in CRPC cells utilize distinct pathways of nuclear import that affect the antitumor efficacy of taxanes, suggesting a mechanistic rationale to customize treatments for patients with CRPC, which might improve outcomes. *Cancer Res; 74(8); 2270–82. ©2014 AACR.*

Introduction

Prostate cancer progression is dependent on continuous androgen receptor signaling and transcriptional activity. Thus, strategies designed to effectively inhibit androgen receptor transcriptional activity and signaling are at the forefront of current research in prostate cancer. The importance of the androgen receptor in prostate cancer disease progression is further highlighted by the fact that many recent therapies are designed to target the androgen axis, such as enzalutamide (formerly MDV3100; refs. 1 and 2), an androgen receptor antagonist, and abiraterone (3), a CYP17 inhibitor that inhibits androgen synthesis. However, resistance to all forms of androgen deprivation therapy (ADT), including these next-generation compounds, occurs eventually and results in disease progression. In fact, despite androgen ablation, the progression to castration-resistant prostate cancer (CRPC) remains androgen receptor driven (4) because of several mechanisms, including androgen receptor gene amplification, *in situ* androgen production (5), the presence of ligand-independent androgen receptor splice variants that localize to the nucleus and are constitutively active (6, 7), and the appearance of the recently identified ligand-binding domain (LBD) mutant form of AR^{F876L} (8, 9).

Following disease progression on ADT, patients with CRPC are commonly treated with taxanes, microtubule-stabilizing drugs, which represent the only class of chemotherapy drugs that prolongs survival in CRPC (10, 11) and are used as standard first- and second-line chemotherapy. We and others have recently shown that androgen receptor signaling is inhibited by taxane treatment, as drug-induced microtubule stabilization abrogates androgen receptor's nuclear translocation and transcriptional activity (12, 13). Specifically, we showed that following ligand stimulation, androgen receptor traffics on microtubules with the aid of the microtubule-based minus-end–directed motor protein dynein, in order to be efficiently trafficked to the nucleus, where it exerts its transcriptional activity (12). Importantly, using patient with CRPC-derived circulating tumor cells, we observed a significant correlation between androgen receptor cytoplasmic sequestration and

Authors' Affiliations: [1]Department of Medicine, Division of Hematology and Medical Oncology, Weill Cornell Medical College; [2]Weill Cornell Cancer Center, New York, New York; [3]Department of Urology, University of Washington; [4]Research Service, Puget Sound VA Health Care System; [5]Department of Medicine, University of Washington; and [6]GRECC Seattle VAMC, Seattle, Washington

Note: Supplementary data for this article are available at Cancer Research Online (http://cancerres.aacrjournals.org/).

M. Thadani-Mulero and L. Portella contributed equally to this work.

Corresponding Author: Paraskevi Giannakakou, Weill Cornell Medical College, 1300 York Avenue-Box 113, New York, NY 10021. Phone: 212-746-3783; Fax: 212-746-6731; E-mail: pag2015@med.cornell.edu

doi: 10.1158/0008-5472.CAN-13-2876

Published OnlineFirst February 20, 2014; DOI: 10.1158/0008-5472.CAN-13-2876

clinical response to taxane chemotherapy. These results demonstrate that androgen receptor inhibition can occur as a result of microtubule stabilization and is a critical mechanism underlying clinical activity of taxanes in prostate cancer (14).

This newly identified mechanism of taxane activity predicts that the combination of taxanes with next-generation androgen receptor targeting drugs would be synergistic because they both inhibit androgen receptor signaling, by targeting different components of androgen receptor signaling axis (14). For example, abiraterone inhibits ligand production, whereas taxanes inhibit the nuclear translocation of the receptor–ligand complex. Despite this prediction, a recent clinical study reported that the activity of docetaxel post-abiraterone was lower than expected whereas no responses to docetaxel were observed in abiraterone-refractory patients (15). These data suggested that perhaps besides the common mechanism of action (inhibition of androgen receptor axis) these 2 classes of drugs, taxanes, and androgen receptor inhibitors, might also share a common mechanism of resistance.

Interestingly recent reports have shown that constitutively active androgen receptor splice variants are overexpressed in CRPC (16–19) and confer resistance to both enzalutamide and abiraterone (20, 21). Androgen receptor variants ARv567 and ARv7 seem to be the 2 most clinically prevalent splice variants, with ARv567 present in 59% of tumor specimens from patients with CRPC (19) and arising in response to ADT or abiraterone treatment (20) and ARv7 present in both benign and malignant prostate tissues but mostly enriched in metastatic disease (17, 22). Together these studies show that the presence of androgen receptor splice variants is common in CRPC and associates with resistance to current androgen deprivation therapies (20, 21).

The impact of androgen receptor variant expression on taxane sensitivity and resistance has not been evaluated. Here, we set out to investigate the mechanisms underlying the variants ARv567 and ARv7 nuclear translocation and constitutive activity, and whether their presence would affect taxane sensitivity. Our results show that ARv567, but not ARv7, utilizes dynamic microtubules and the dynein motor protein for its nuclear accumulation and resultant transcriptional activity and as such only taxane treatment sequesters ARv567 "inactive" in the cytoplasm, whereas it has no effect on ARv7 subcellular localization and nuclear activity. We have also identified the minimum microtubule-binding domain on the androgen receptor, which lies within the DNA-binding domain and the hinge region. Interestingly, ARv7, which does not display microtubule-binding properties lacks the hinge region and thus lacks the main part of the bipartite nuclear localization signal (NLS; refs. 23–26). We show that ARv567 expression confers docetaxel sensitivity *in vivo*, whereas expression of the microtubule-independent ARv7 variant confers resistance. Taken together, our data identify distinct mechanisms of cytoplasmic to nuclear trafficking for the 2 androgen receptor variants, which underlie their differential sensitivity to taxane treatment, suggesting that variant expression could be used as a potential predictive biomarker of taxane clinical activity in CRPC.

Materials and Methods

Cell lines and reagents

PC3 and HEK293T cells were obtained from American Type Culture Collection and a PC3 stable cell line expressing mCherry-tubulin (PC3:mCherry-tub) was generated and maintained as previously described (12).

M12 cell line is derived by human prostate epithelial cells immortalized with the SV40T antigen to produce the poorly tumorigenic P69SV40T cell line. After injection into athymic nude mice the produced tumor nodules were reimplanted in athymic mice, leading to the generation of the M12 cells, which demonstrated a shorter latency period to tumor formation and were locally invasive and metastatic compared with the initial P69SV40T. We chose M12 cells for subsequent transfection experiments with GFP-tagged AR-wt or androgen receptor variants as they do not express endogenous AR protein. GFP^+ cells from all 3 androgen receptor cell lines were sorted using fluorescence-activated cell sorting (FACS) on a BD FACSAria II cell sorter (BD Biosciences) and subsequently expanded in media containing G418 (400 ng/mL).

M12 stable cell lines expressing untagged wild-type androgen receptor (AR-wt), ARv567es and ARv7 or expressing Cumate-inducible FLAG-tagged AR-wt or variants were generated in Dr. Plymate's laboratory (University of Washington School of Medicine) and maintained in RPMI 1640 supplemented with 5% FBS, 0.01 μmol/L dexamethasone (Sigma Aldrich), 10 ng/mL epidermal growth factor (Invitrogen), 10 ml/L insulin–transferrin–selenium (Cellgro), 100 IU/mL penicillin plus 100 μg/μL streptomycin at 37°C with 5% CO_2.

Unless otherwise stated, all reagents used were from Sigma Aldrich. For immunofluorescence, we used the following primary and secondary antibodies: rat monoclonal anti-α-tubulin (Novus Biologicals), rabbit polyclonal anti-AR-N21 developed in our lab using as an antigen the first 21 amino acids of androgen receptor and species-matching Alexa Fluor 488 and Alexa Fluor 568 conjugated antibodies from Invitrogen. For immunoprecipitation we used rat monoclonal anti α-tubulin, rabbit polyclonal anti-GFP (Novus Biologicals) and mouse anti-dynein (Covance) antibodies. For the immunoblot assays, we used mouse monoclonal anti-AR 441 (Novus Biologicals); rabbit monoclonal anti-AR (EP670Y from Abcam) specific for the C-terminus; mouse monoclonal anti-ARv7 (Precision Antibody) specific for ARv7 variant; mouse monoclonal anti-FLAG M2 (Sigma Aldrich); rat monoclonal anti-α-tubulin; rabbit polyclonal anti-GFP (Abcam); and rabbit polyclonal anti-actin (Sigma Aldrich) antibodies. Alexa Fluor 680 (Invitrogen) and IRDye 800 (Rockland) conjugated antibodies were as secondary antibodies. Methyltrienolone (R1881) and Paclitaxel were purchased from Sigma Aldrich and docetaxel from Sanofi Aventis.

Generation of AR truncated mutants

The full-length GFP-AR plasmid (pEGFP-C1-AR-Q22) was generously provided by Dr. M. Mancini (Baylor College of Medicine, Houston, TX) and used as the template to generate all androgen receptor–truncated mutant constructs. All PCR-generated androgen receptor–truncated mutant constructs were subcloned into the expression vector pEGFP-C1. All

Published OnlineFirst February 20, 2014; DOI: 10.1158/0008-5472.CAN-13-2876

Table 1. Primers used to generate androgen receptor–truncated mutant constructs

Segment	Forward	Reverse
Androgen receptor N-terminal domain	5′-cgcgtcgacatggaagtgcagttagggctg-3′	5′-cgggatcctcacgcatgtccccgtaaggt-3′
Androgen receptor C-terminal domain	5′-cgcgtcgacatgcgtttggagactgccag-3′	5′-cgggatcctcactgggtgtggaaatagatggg-3′
Androgen receptor 540-558	5′-cgcacgaattctatgttggagactgccagggacc-3′	5′-cgcacggatcctcacttctggggtggaaagtaatag-3′
Androgen receptor 559-624 (DBD)	5′-cgcacgaattctatgacctgcctgatctgtggag-3′	5′-cgcacggatcctcaccctgcttcataacatttccg-3′
Androgen receptor 559-663 (DBD-Hinge)	5′-cgcacgaattctatgacctgcctgatctgtggag-3′	5′-cgcacggatcctcatgacactgtcagcttctggg-3′
Androgen receptor 624-663 (Hinge)	5′-cgcacgaattctatgactctgggagcccgg-3′	5′-cgcacggatcctcatgacactgtcagcttctggg-3′
Androgen receptor 664-724	5′-cgcacgaattctatgcacattgaaggctatgaatgtc-3′	5′-cgcacggatcctcaaggcaaggccttggcccac-3′

cloning was performed using AccuPrime Taq DNA Polymerase High Fidelity (Invitrogen), with 10 μmol/L forward and reverse cloning primers (IDT). All primers were designed using the human androgen receptor mRNA reference sequence (GenBank NM_000044) and are shown in Table 1.

AR 540-724 and AR 725-919 were subcloned into the p3xFLAG-CMV-14 expression vector (Sigma) with the following specific primers: AR 540-724 forward: 5′-cgcacgatatcgccaccatgttggagactgccagggacc-3′; reverse: 5′-cgcacggatccaggcaaggccttggcccac-3′ and AR 725-919 forward: 5′-cgcacgatatcgccaccatgggcttccgcaacttacacgtg-3′; reverse: 5′-cgcacggatccctgggtgtggaaatagatggg-3′. Amplification products were analyzed by Sanger sequencing to confirm the integrity of all constructs.

Immunoprecipitation and Western Blotting

HEK293T cells transiently transfected with GFP-tagged AR-wt AR, ARv567, or ARv7 were lysed in TNES buffer and subjected to immunoprecipitation as previously described (12).

Microtubule co-sedimentation assay

PC3-mCherry-tubulin and HEK293T cells were transiently transfected with GFP-tagged AR-wt or GFP-ARv7 or HA-tagged ARv567 and subjected to microtubule co-sedimentation assay as previously described (27). Cells were grown in RPMI 10% FBS + 1% P/S till transfection in which the media were replaced with CSS media. No R1881 was added. For the co-sedimentation assay, briefly, 1 mg of total cell lysate was first precleared by high-speed centrifugation. The pellet (HSP) containing mostly insoluble cell debris was discarded after loading a small amount on the gel to identify whether there was significant loss of androgen receptor in the cell debris, whereas the supernatant (HSS) was supplemented with exogenous purified bovine brain tubulin (Cytoskeleton) reconstituted at a final concentration of 10 μmol/L in the presence of 1 mmol/L GTP, and 20 μmol/L paclitaxel (PTX) and subjected to a cycle of polymerization for 30 minutes at 37°C. Samples were centrifuged at 100,000 × *g* for 30 minutes at room temperature and the warm supernatant (WS) was separated from the warm pellet (WP), which was resuspended in an equal volume of PEM buffer. Equal volumes from each respective fraction were loaded onto a SDS-PAGE and transferred and immunoblotted with antibodies against GFP, androgen receptor, α-tubulin, and actin.

Densitometry for each respective protein was performed using ImageJ (NIH) software and the percentage of the protein present in the pellet fraction was calculated using the following formula: $\% P = 100 \times \mathrm{WP}/(\mathrm{WP} + \mathrm{WS})$.

Quantitative real-time PCR

M12-cumate inducible AR-wt or variant cells were treated with cumate (Cu) for 48 hours and then starved for 24 hours in CSS media. Cells were treated with 1 μmol/L docetaxel for 4 hours either alone or followed by 10 nmol/L R1881 overnight. qPCR for TMPRSS2, FKBP51, and glyceraldehyde-3-phosphate dehydrogenase (GAPDH) was performed as previously described (28).

Dynamitin overexpression, immunofluorescence, and confocal microscopy

M12 cells stably expressing the untagged androgen receptor constructs were transiently transfected with c-myc–tagged pCMVH50m plasmid containing dynamitin (gifted by R. Vallee, Columbia University, New York, NY) using FuGENE 6, according to the manufacturer's instructions. Twenty-four hours posttransfection, the cells were treated with the indicated drugs. Images were acquired by confocal microscopy and image analysis was performed as previously described (12).

Live cell imaging

PC3-mCherry-tubulin cells were plated on MatTek 5 mm, poly-D-lysine coated glass bottom dishes and allowed to adhere overnight. Cells were maintained in charcoal-stripped RPMI 1640 at 37°C and 5% CO_2 for 1 hour, pressure-microinjected intranuclearly with plasmids encoding the different GFP-AR cDNAs as previously described (12) and then treated post-microinjection for 2 hours with docetaxel or Noc to affect microtubules. After protein expression, time-lapse images were taken using a Spinning Disk microscopy system consisting of a Zeiss Axiovert 200 system fitted with a Yokogawa CSU-X1 spinning disk head. Time lapse microscopy and image analyses were performed as previously described (12).

Xenograft tumors

LuCaP human prostate cancer xenografts were grown as previously described (20, 29) in noncastrate SCID mice. Briefly, when the tumor volume reached an estimated size of 200 mm^3 ($l \times w^2/2$), mice was treated with either vehicle or docetaxel 5 or 20-mgm/kg i.p. weekly until tumors in the control group

Published OnlineFirst February 20, 2014; DOI: 10.1158/0008-5472.CAN-13-2876

reached a tumor volume of 1,000 mm^3. At this time, all animals in a group were sacrificed. The LuCaP 23.1 and LuCaP 86.2 prostate cancer xenograft lines were developed by coauthor RLV at the University of Washington. The preclinical studies presented here were performed in his laboratory. All animal studies were approved by the University of Washington Institutional Animal Care and Use Committee.

Immunohistochemistry

Androgen receptor immunostaining of explanted LuCaP tumors was conducted as previously described (30).

Statistical analysis

The *P* values for androgen receptor nuclear localization in control-, taxane-, and nocodazole-treated cells were calculated using one-way ANOVA followed by multiple comparisons with Bonferroni adjustments using Stata Statistical Software: release 10. The *P* value for androgen receptor nuclear versus cytoplasmic localization in M12 cells were calculated using 2-tailed unpaired *t* test.

Image analysis

For all images, segmentation of the nuclei and the cellular area was done using MATLAB, MathWorks. Using the 4′,6-diamidino-2-phenylindole images, we applied a unimodal thresholding algorithm (31) to identify the nuclear areas for each cell. We then computed the total intensity for the nuclear areas in the androgen receptor images and obtained the overall androgen receptor nuclear intensity for each cell. We used the coordinates of the centroids of the nuclei to build a Voronoi diagram (32) and identify the approximate area of the cytoplasm for each cell. We then computed the total intensity in the androgen receptor images for each cellular area, including the cytoplasmic and nuclear areas. The percentage of androgen receptor nuclear accumulation was calculated as the ratio of the nuclear to cellular androgen receptor for each individual cell.

Results

Microtubule binding is mediated by the C-terminal domain of the androgen receptor

We have previously shown that wild-type androgen receptor (AR-wt) associates with the microtubule cytoskeleton and that this association is important for androgen receptor cytoplasmic to nuclear translocation and transcriptional activity in CRPC (12, 14). However, the androgen receptor protein domain required for microtubule association remains unknown. To determine the microtubule binding domain on the androgen receptor protein, we performed a microtubule co-sedimentation assay using cells expressing overlapping truncated androgen receptor mutants, which we generated by a serial mutagenesis approach. The microtubule co-sedimentation assay is an assay routinely used to analyze proteins that specifically bind to microtubule polymers. The basic principles of the assay involve addition of exogenous purified microtubule protein to a crude cell extract, which is then subjected to a cycle of polymerization in the presence of the microtubule-stabilizing drug paclitaxel. Any cellular proteins that have affinity for the microtubule polymer will co-sediment with the tubulin pellet following ultracentrifugation at 100,000 $\times$ *g*. Following centrifugation, the pellet (microtubules and associated cell proteins) and supernatant (soluble tubulin dimers and all other cell proteins) fractions are loaded on adjacent wells of an SDS-PAGE, transferred and immunoblotted for the proteins of interest.

Initially, 2 large androgen receptor truncations were generated and subcloned into a pEGFP-C1 vector: the N-terminal domain (N-ter, aa 1-539) encompassing exon 1 of the androgen receptor and the C-terminal domain (C-ter, aa 540-919) encompassing the DNA binding domain, the hinge region and the ligand binding domain of androgen receptor (Fig. 1A). Each deletion mutant was individually expressed in either PC3: mCherry-tub or HEK293T cells by transient transfection and cells were subjected to microtubule co-sedimentation in order to assess each proteins' association with microtubule polymers. In this assay, cell lysates from each condition (HSS) were supplemented with exogenous purified tubulin and subjected to a cycle of microtubule polymerization at 37°C and in the presence of GTP and Taxol. Under these conditions, purified tubulin along with endogenous cellular tubulin is robustly polymerized enabling microtubule interactions with cellular proteins. Following the polymerization reaction, high-speed centrifugation separates microtubule polymers along with any cellular proteins with affinity for them into the WP fraction, whereas soluble tubulin and other proteins that do not have affinity for microtubules segregate with the WS. The distribution of androgen receptor proteins between the WP and WS fractions indicates its ability to associate with the microtubule polymers. Efficient tubulin polymerization was observed in all conditions.

Our results revealed that the C-terminal domain of GFP associated preferentially with microtubule polymers in both cell lines (Figs. 1B and Supplementary Fig. S1), as 86% of the C-ter AR cofractionated with microtubules in the WP fraction, similar to the AR-wt. In contrast, N-ter AR showed minimal association (13%) with polymerized tubulin (Figs. 1B and Supplementary Fig. S1). Tubulin was efficiently polymerized in all conditions as shown by the majority of tubulin (over 80%) found in respective WP fractions.

To further narrow down the minimum androgen receptor microtubule binding domain, we generated 7 additional androgen receptor truncation mutants within the C-ter region of androgen receptor (Fig. 1C). The truncations were designed to correspond to androgen receptor functional domains as well as to cover the entire C-ter region, as follows: the DNA binding domain (aa 559-624), the hinge region (aa 625-663), the DNA binding domain plus the hinge region (aa 559-663), and fragments aa 540-724, 540-558, 664-724, and 725-919. These deletion mutants were subcloned into a pEGFP-C1 vector, with the exception of aa 540-724 and 725-919 mutants, which were subcloned into a p3XFLAG-CMV vector as the GFP-tag gave rise to a protein of approximately 50 kDa, which is also the size of tubulin, whose excess made the detection of the truncated proteins very challenging. Of the 7 truncation mutants, the AR 559-663, corresponding to the DNA BD plus the hinge region, showed the most extensive association with the microtubule

Published OnlineFirst February 20, 2014; DOI: 10.1158/0008-5472.CAN-13-2876

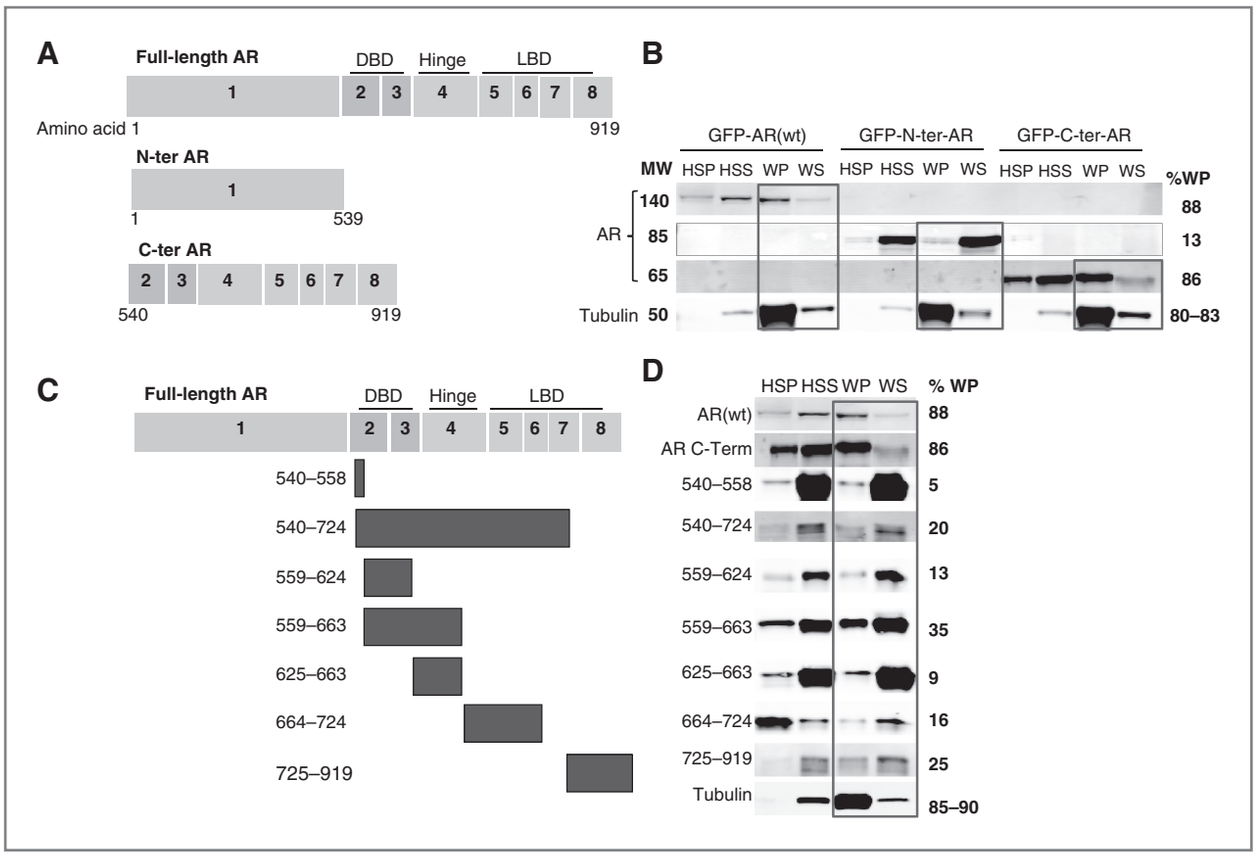

Figure 1. Microtubule binding is mediated by the C-terminal domain of androgen receptor (AR). A and C, schematic representation of androgen receptor deletion mutants as indicated. B and D, microtubule co-sedimentation assay of PC3:mCh-tub cells transiently expressing GFP-AR(wt), GFP-N-terminal androgen receptor (N-ter AR), or GFP-C-terminal androgen receptor (C-ter AR) or each of the smaller deletion mutants as indicated. Cell lysates from each condition (HSS) were supplemented with exogenous tubulin and subjected to microtubule polymerization in the presence of GTP and paclitaxel. The samples were centrifuged at 100,000 $\times$ *g* to separate the microtubule polymers (WP) from the soluble tubulin dimers (WS), resolved by SDS-PAGE, and immunoblotted for the presence of androgen receptor and tubulin as indicated. HSP, high-speed pellet containing cellular proteins that aggregated nonspecifically. HSS, high-speed supernatant (cell lysate). WP, warm pellet containing microtubule polymers and associated proteins. WS, warm supernatant containing soluble tubulin dimers and proteins not associated with microtubules. Boxes highlight the relative protein distribution between the WP and WS fractions from each condition. The percent protein present in the pellet fraction (%WP) was calculated using the following formula: $\%P = 100 \times \mathrm{WP}/(\mathrm{WP} + \mathrm{WS})$ and is presented to the right of each immunoblot. For tubulin a range of values is shown in the %WP quantitation reflecting each of the 3 reactions performed. The blots shown in B belong to the same gel, which was blotted with anti-AR 441 for AR-wt and N-terminal androgen receptor, and anti-androgen receptor (EP670Y) specific for the C-terminal androgen receptor, anti-tubulin and anti-actin antibodies. In D, all androgen receptor deletion mutants were detected with an anti-GFP antibody except for the androgen receptor 540–724 and androgen receptor 725–919 deletion mutants that were detected with an anti-FLAG antibody.

polymers with 35% protein seen in the WP (Fig. 1D). Surprisingly, none of these androgen receptor deletion mutants showed as extensive association with the microtubule polymer fraction as the original C-ter AR (Fig. 1B), suggesting that likely there is contribution from different parts of the androgen receptor within its C-terminus region for effective tubulin association.

ARv567 associates more extensively with microtubules compared with ARv7

We then sought to investigate whether any of the 2 most clinically prevalent androgen receptor splice variants with truncations in their C-terminus, namely ARv567 (19) and ARv7 (17, 18), would associate with microtubules similar to the AR-wt. Microtubule co-sedimentation revealed that the ARv567 variant cofractionated almost exclusively (70%) with microtubule polymers in the WP fraction, whereas ARv7 only partially cofractionated with microtubules at 42% (Fig. 2B).

ARv567, but not ARv7, nuclear translocation is impaired by microtubules targeting drugs

The distinct pattern of microtubule association exhibited by the 2 androgen receptor variants suggested potentially distinct mechanisms of nuclear translocation. To test this hypothesis, we perturbed the microtubule network by 2-hour treatment with drugs that either stabilize (docetaxel) or depolymerize (nocodazole) microtubules and assessed androgen receptor variant nuclear accumulation in cells microinjected with GFP-tagged ARv567 or ARv7. Live cell confocal microscopy was then used to image the dynamics of androgen receptor variant

Published OnlineFirst February 20, 2014; DOI: 10.1158/0008-5472.CAN-13-2876

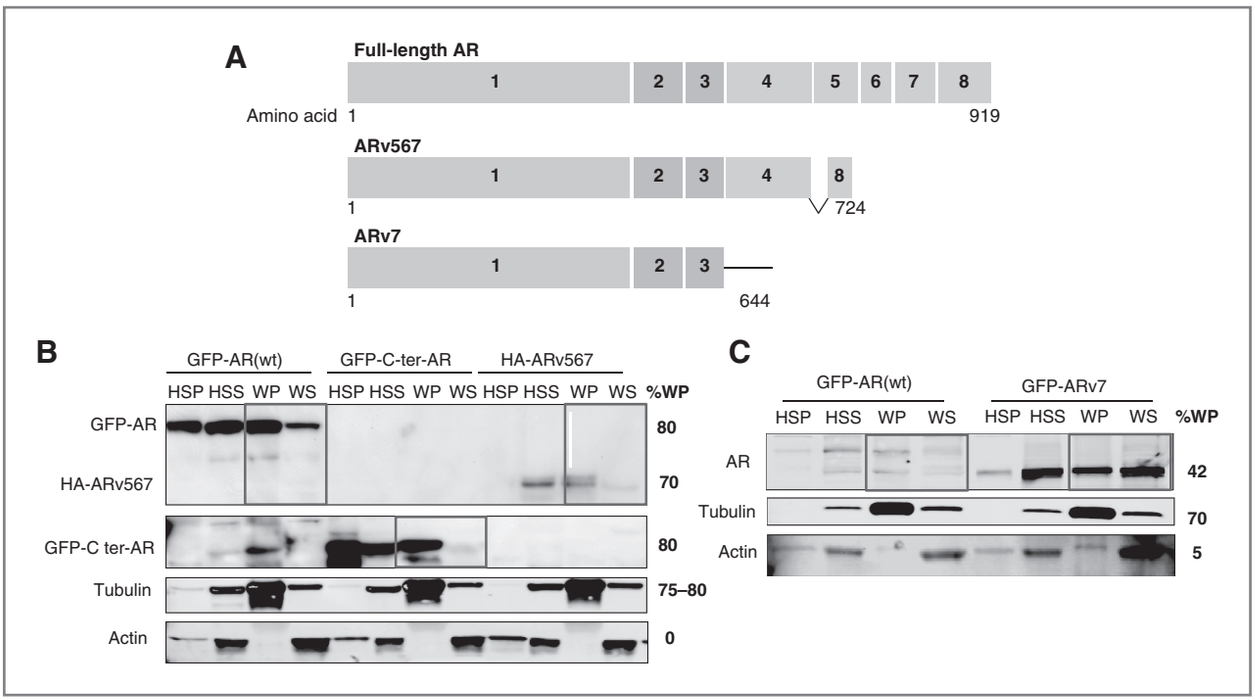

Figure 2. ARv567, but not ARv7, associates with the microtubule polymer. A, schematic representation of full-length androgen receptor as well as the splice variants ARv567, encoding exons 1–4 and the first 10 amino acids of exon 8, and ARv7, encoding exons 1–3 and a cryptic exon of 16 amino acids. B and C, A microtubule co-sedimentation assay using whole cell lysate (HSS) from PC3:mCh-tub cells transfected with either GFP-AR (wt), HA-ARv567, or GFP-ARv7 was carried out as in Fig. 1. AR-wt androgen receptor was used as positive controls of microtubule binding. Proteins from each of the fractions were immunoblotted using anti–androgen receptor specific for the C-terminus (EP670Y) to detect GFP-AR-C-ter; anti-AR 441 to detect GFP-AR (wt), HA-ARv567 and GFP-ARv7; anti-tubulin and anti-actin antibodies. Tubulin was detected as microtubules in the WP in each condition. Boxes indicate the distribution of each protein between WP and WS fractions per condition. The extent of each variant's association with the microtubule polymer (%WP) was quantified by densitometry as in Fig. 1 and is displayed to the right of each immunoblot. For tubulin, a range of values is shown in the %WP quantitation, reflecting each of the 8 reactions performed. Actin was used as a negative control for microtubule association and is found in the supernatant fractions (WS) in all conditions.

nuclear accumulation by obtaining z-stack images every 10 minutes for a total of 120 min.

Representative images from each condition are shown in Fig. 3 and reveal that the nuclear accumulation of ARv567 was significantly impaired following microtubule perturbation with either drug, while ARv7 remained largely unaffected in the nucleus (see movies in Supplement). Interestingly, and in agreement with published reports (17–19, 33), the 2 variants were found predominantly in the nucleus of untreated cells as soon as the GFP-tagged protein was expressed following microinjection (time 0). Despite their initial nuclear localization at baseline, the 2 variants exhibited entirely distinct responses to drug-induced microtubule disruption. Quantitation of the extent of nuclear ARv567 revealed a significant decrease in its nuclear localization following microtubule perturbation at all time points tested (Fig. 3C and Supplementary Table S1 $P < 0.01$ at baseline and $P < 0.001$ at all other time points). The integrity of the microtubule cytoskeleton was assessed in each condition before time lapse image acquisition and is shown in the right panels of the figure, indicating effective drug-target engagement for each of the conditions, microtubule bundling with docetaxel (Fig. 3A and B, middle row, arrowhead) and depolymerized tubulin with nocodazole treatment (Fig. 3A and B,, third row). In contrast and despite effective drug-target engagement, drug treatment had no effect on the other clinically relevant and constitutively active androgen receptor splice variant, ARv7 (18). Treatment of the ARv7-microinjected cells with microtubule targeting drugs did not impact this variant's nuclear localization at any time point (Fig. 3B and D and Supplementary Table S1). Taken together, these data suggested that ARv567 but not ARv7 is dependent on microtubules for effective nuclear accumulation.

To extend these observations, we used the M12 prostate cancer cell line, a tumorigenic cell line representative of the metastatic stage of prostate cancer, to engineer isogenic cell lines stably expressing GFP-tagged AR-wt AR, ARv567, or ARv7. We then investigated the effects of docetaxel treatment on the nuclear localization of each of the GFP-tagged receptors, as seen by GFP fluorescence (Fig. 4A and B) or antibody-based detection (Supplementary Fig. S2). In agreement with our previous data (12), docetaxel inhibited ligand-induced AR-wt nuclear accumulation downstream of microtubule stabilization (Fig. 4A, arrowhead for microtubule bundles, arrows for cytoplasmic androgen receptor). Docetaxel treatment also inhibited the nuclear localization of the ligand-independent ARv567 variant (Fig. 4B). Similar results were obtained in the presence of R1881, which did not induce any further nuclear accumulation of ARv567 (Supplementary Fig. S3A). However, as shown in Fig. 4C, docetaxel treatment failed to alter the nuclear localization of ARv7 variant in the absence or presence

Published OnlineFirst February 20, 2014; DOI: 10.1158/0008-5472.CAN-13-2876

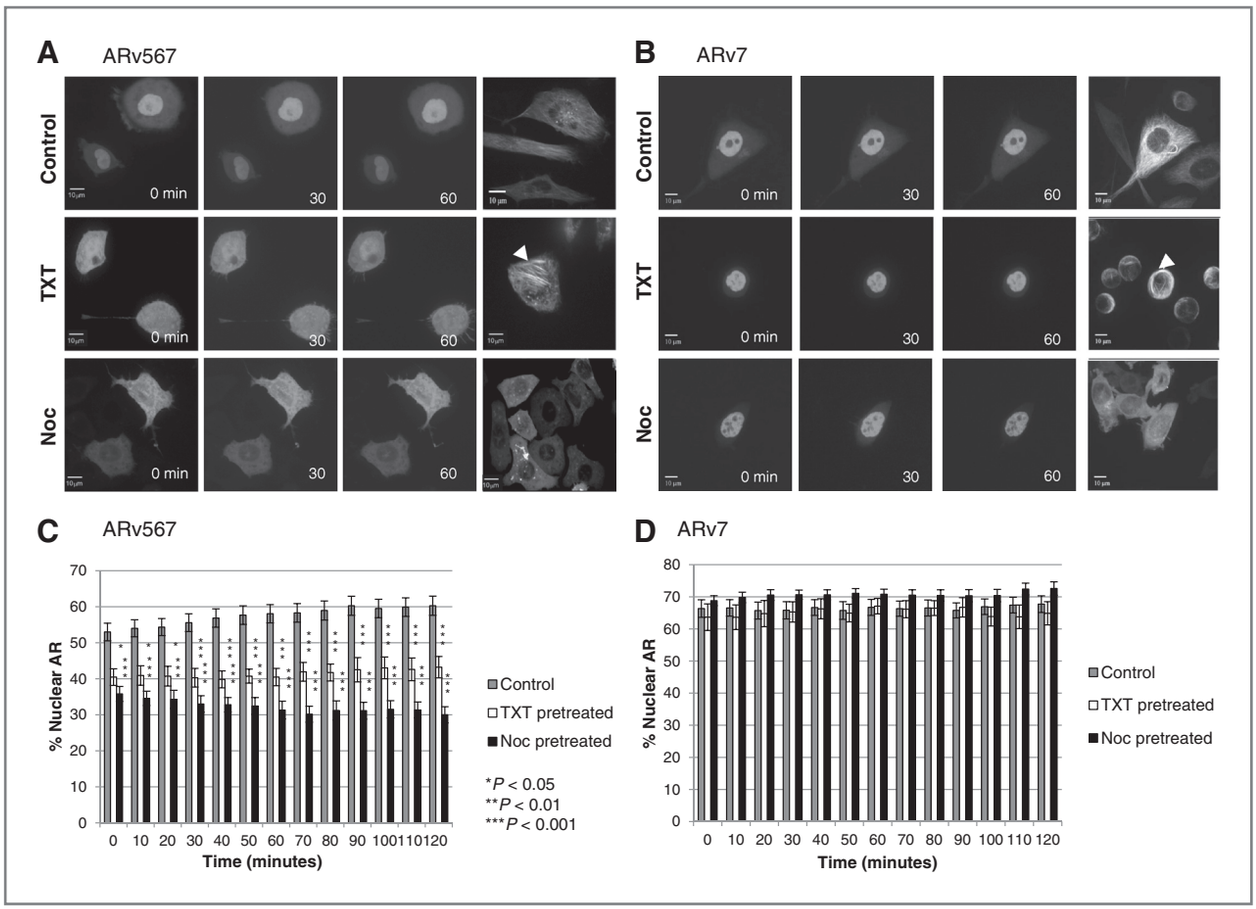

Figure 3. Microtubule targeting drugs inhibit ARv567 nuclear trafficking but have no effect on ARv7 nuclear accumulation. PC3:mCh-tub cells were microinjected with GFP-tagged ARv567 or GFP-tagged ARv7 and incubated for 2-hour post-microinjection with either 1 μmol/L docetaxel (TXT) or 10 μmol/L nocodazole (Noc). Time lapse images were obtained with a spinning disk confocal microscope by acquiring an entire Z-stack at 10-minute intervals for 2 hours. Shown are maximum intensity projections of representative PC3: mCherry-Tub cells expressing GFP-ARv567 (A) or GFP-ARv7 (B) at the indicated time points (movies in supplement). The integrity of the microtubule cytoskeleton from untreated, docetaxel, or Noc-treated cells was visualized with mCherry-tagged tubulin at the beginning of the time lapse recording and is shown in the far right panels. Arrowhead, microtubule bundles. C and D, graphic representation of ARv567 (C) or ARv7 (D) nuclear accumulation over time following treatment in control versus docetaxel- and Noc-pretreated cells. Quantitative analysis of nuclear of GFP-AR was performed on each focal plane (0.5 μm Z-sections through the entire cell depth) using integrated pixel intensity values from the sum projection and the percentage of nuclear androgen receptor was calculated using the following formula: % nuclear androgen receptor = 100 × nuclear androgen receptor/total androgen receptor. Number of individual cells imaged per condition (*n*) ARv567: Control 0, 10, 20, and 30 minutes: $n = 16$; 40 to 120 minutes: $n = 15$. Docetaxel pretreated 0 to 80 minutes: $n = 12$; 90–120 minutes: $n = 10$. Noc pretreated 0–50 minutes: $n = 11$; 60 to 110 minutes: $n = 10$; 120 minutes: $n = 3$. *N* values for ARv7: Control 0 to 120 minutes: $n = 9$. Docetaxel pretreated 0 to 120 minutes: $n = 9$. Noc pretreated 0 to 100 minutes: $n = 21$, 110 to 120 minutes: $n = 7$. Statistical test: one-way ANOVA with equal variances followed by multiple comparisons with Bonferroni adjustments.

of R1881 (Supplementary Fig. S3B). In addition, we quantified the extent of androgen receptor nuclear localization for each condition by calculating the ratio of nuclear to total cellular androgen receptor for each individual cell, as described in the Materials and Methods (Fig. 4D). This analysis revealed that docetaxel treatment resulted in a significant decrease of nuclear localization in AR-wt and ARv567, but had no effect on ARv7 confirming and corroborating the live cell imaging results that showed that ARv7 does not depend on microtubules for its nuclear trafficking. To assess the effect of docetaxel treatment on androgen receptor transcriptional activity, we performed quantitative real-time PCR using transcriptional targets previously shown to be differentially induced by AR-wt and androgen receptor variants. Specifically, TMPRSS2 was identified as a target specific for AR-wt whereas FKBP51 was transcriptionally activated by the androgen receptor variants (18, 34). In this assay, we used M12 cells expressing inducible AR-wt or variants. As seen in Fig. 4E, in M12 cells, the AR-wt increased TMPRSS2 expression and docetaxel treatment significantly inhibited it, consistent with the drug's effects on androgen receptor cytoplasmic sequestration. In the case of the androgen receptor variants, TMPRSS2 is no longer regulated whereas FKBP51 transcription is induced by both ARv7 and ARv567. Here we see that docetaxel treatment significantly inhibited ARv567-mediated induction of FKBP51 but had no effect on ARv7 transcriptional activity, in agreement with the differential effects of docetaxel on each variant's nuclear localization (Fig. 4B and C). These data confirm that the

Published OnlineFirst February 20, 2014; DOI: 10.1158/0008-5472.CAN-13-2876

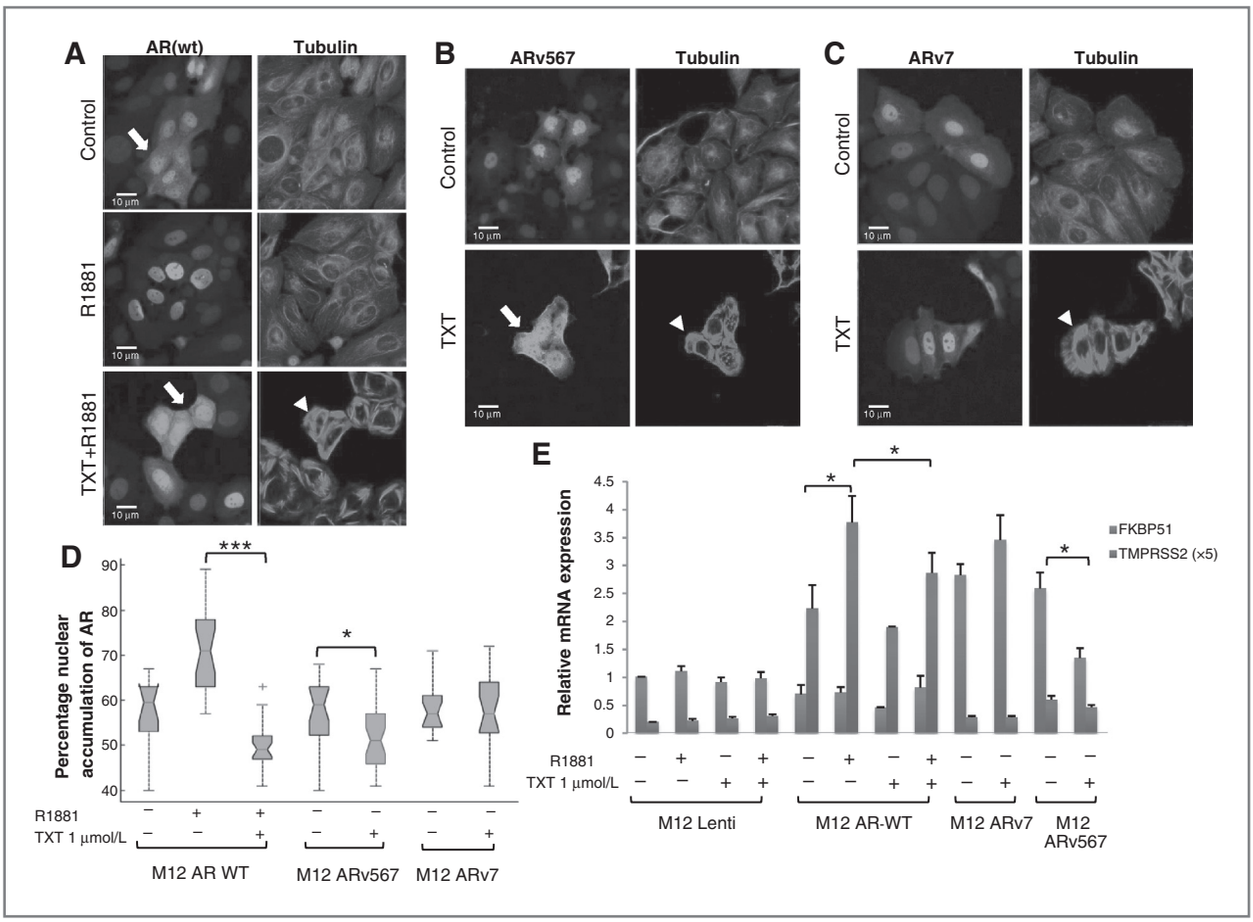

Figure 4. Taxane treatment inhibits AR-wt androgen receptor and ARv567, but not ARv7, trafficking to the nucleus in M12 cells. A–C, M12 cells stably expressing GFP-tagged AR-wt androgen receptor (A), ARv567 (B), and ARv7 (C) were treated with 1 μmol/L docetaxel (TXT) for 4 hours either alone or followed by 10 nmol/L R1881 for 2 hours as indicated in the figure. Cells were then fixed, immunostained for tubulin, and imaged for GFP-AR and tubulin by confocal microscopy. Representative, high-magnification images from each condition are shown. Arrows, cytoplasmic androgen receptor; arrowheads , microtubule bundles. Scale bar, 10 μm. D, for each condition, at least 20 representative cells expressing either AR-wt or each androgen receptor variant were analyzed. Box plots indicate the 25th percentile (bottom boundary), median (middle line), 75th percentile (top boundary), nearest observations within the interquartile range (whiskers); whiskers extend to 1.5× the interquartile range; dots indicate outliers beyond this range. Notched boxes indicate uncertainty of the median. ***, significance of the difference between the two conditions with $P < 0.005$. *, significance of the difference between the two conditions with $P < 0.05$. E, M12 cells expressing inducible AR-wt or androgen receptor variants were treated with 1 μmol/L docetaxel (TXT) for 4 hours either alone or followed by 10 nmol/L R1881 overnight as indicated in the figure. Relative mRNA expression of TMPRSS2 and FKBP51 was assessed by qPCR. Values were corrected to GAPDH and normalized to untreated M12 cells expressing control lentivirus (M12 lenti). Bar graphs represent the average of three independent experiments. *, $P < 0.05$.

androgen receptor variants have a distinct transcriptome compared with AR-wt but that nuclear localization is necessary for AR-V and AR-wt activity.

Dynamitin overexpression impairs ARv567 nuclear translocation, whereas it has no effect on ARv7

To further dissect the mechanism regulating the cytoplasmic to nuclear translocation of each variant, we next investigated the involvement of the minus-end directed microtubule motor protein dynein, because we have shown that it mediates nuclear translocation (12). Dynein works in concert with several accessory proteins to drive subcellular motile functions, including dynactin, which is an adapter that mediates the binding of dynein to cargo structures enhancing dynein's motor function. Overexpression of the dynactin-associated protein, dynamitin, which disrupts dynein–cargo interactions (35), was used to dissect the involvement of dynein in the transport of the androgen receptor splice variants to the nucleus.

M12 cells stably expressing untagged ARv567 (M12-ARv567) or ARv7 (M12-ARv7) were transiently transfected with a c-myc–tagged p50-dynamitin vector and processed for double-labeling immunofluorescence with anti-AR and anti-c-myc antibodies. Overexpression of dynamitin impaired nuclear accumulation of ARv567 (Fig. 5A, dashed arrows point to cytoplasmic androgen receptor) but had no effect on the nuclear accumulation of ARv7 (Fig. 5B arrows point to nuclear androgen receptor). Quantitation of the extent of androgen receptor nuclear accumulation revealed a significant decrease of ARv567 in the nucleus of

Published OnlineFirst February 20, 2014; DOI: 10.1158/0008-5472.CAN-13-2876

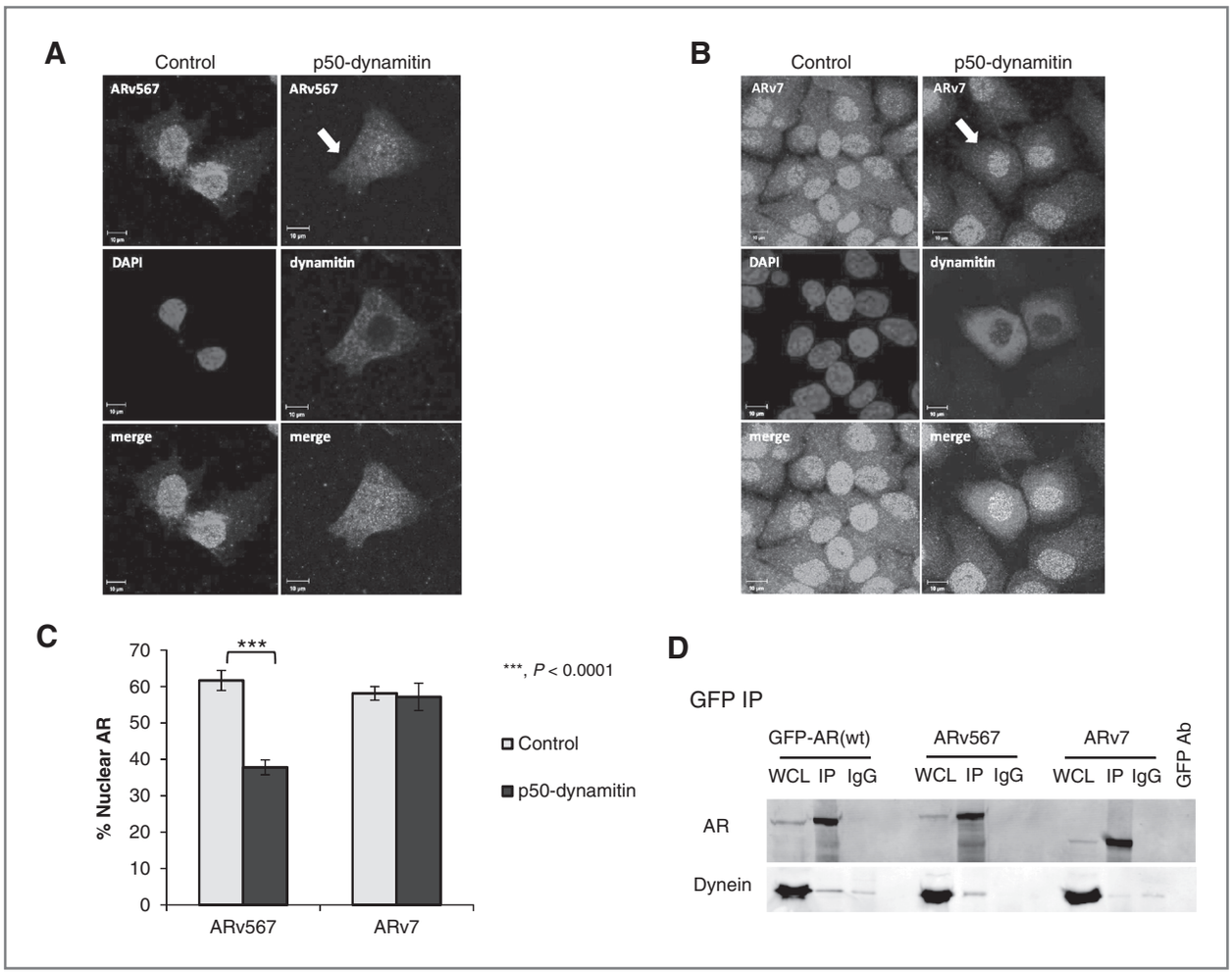

Figure 5. Dynein associates with and mediates the nuclear translocation of ARv567, but not ARv7. M12 cells stably expressing untagged androgen receptor variants, M12-ARv567 (A) and M12-ARv7 (B), were transiently transfected with pCMVH50myc (encoding a c-myc–tagged human dynamitin). Cells were fixed, processed for double immunoflourescence labeling with anti-androgen receptor and c-myc antibodies, and analyzed by confocal microscopy. Solid arrows, nuclear androgen receptor. C, quantitation of the amount of each of the variants in the nucleus was performed using MetaMorph image analysis software and shows a marked decrease of nuclear ARv567 after dynein-cargo disruption. ARv7, however, remains unaffected by dynamitin overexpression. The number of cells examined for each experimental condition is as follows: ARv567 CTL, 9 cells; ARv567 p50-dynamitin, 18 cells; ARv7 CTL, 28 cells; ARv7 p50-dynamitin, 10 cells. D, 1 mg input whole cell lystate from 293T cells transiently transfected with GFP-AR(wt), GFP-ARv567, and GFP-ARv7 were immunoprecipitated with a GFP antibody or control IgG and immunoblotted for dynein and androgen receptor. Fifty micrograms of WCL was loaded as input. One microliter of GFP antibody was loaded onto the gel as a control for the size of heavy chains in the samples.

dynamitin expressing cells as compared with dynamitin-overexpressing M12-ARv7 cells, where no effect on nuclear ARv7 was observed (Fig. 5C).

To further investigate the role of the dynein microtubule-based motor protein on androgen receptor variant trafficking, we performed a co-immunoprecipitation experiment in HEK293T cells transiently transfected with GFP-tagged AR-wt AR, ARv567, or ARv7 to determine their putative association with dynein. Co-precipitation using an antibody against GFP revealed that both the AR-wt AR and ARv567, but not ARv7, associated with dynein (Fig. 5D). Taken together, these data support a model whereby AR-wt AR and ARv567 utilize microtubules and dynein-dependent transport for their nuclear accumulation and subsequent activity. However, ARv7 does not utilize this mechanism of transport and hence remains insensitive to taxane treatment.

Docetaxel treatment inhibits ARv567-mediated subcutaneous tumor growth in SCID mice

Our recent (12, 14) and current data suggest that inhibition of androgen receptor nuclear accumulation and transcriptional activity mediates, as least in part, the clinical activity of taxanes. To determine the impact of androgen receptor variant expression on taxane sensitivity *in vivo*, we compared the effects of docetaxel on the growth of 2 LuCaP xenograft tumors grown subcutaneously in SCID mice as described in Materials and Methods. The tumors were LuCaP 86.2, a human xenograft tumor in which the majority of the androgen receptor is

Published OnlineFirst February 20, 2014; DOI: 10.1158/0008-5472.CAN-13-2876

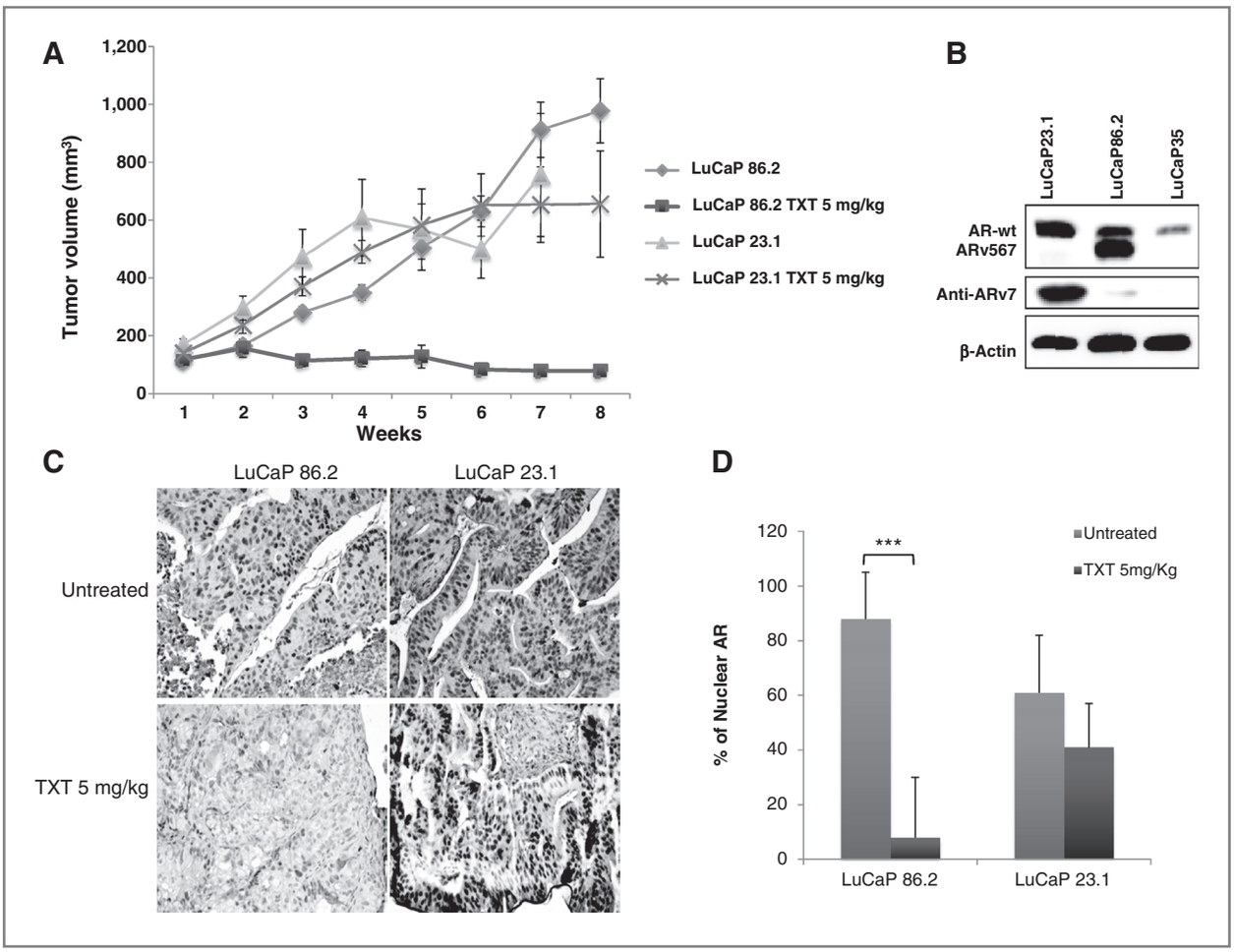

Figure 6. Docetaxel (TXT) treatment inhibits ARv567-mediated subcutaneous tumor growth in SCID mice. A, human prostate cancer xenografts LuCap 86.2, expressing predominantly ARv567, and LuCap 23.12 expressing both AR(wt) and ARv7, were treated with docetaxel 5 mg/kg weekly intraperitoneal or vehicle control. Study was terminated when all mice in the LuCaP 23.1 5 mg/kg group met UW IACUC criteria for euthanasia. *Y*-axis shows tumor volumes ± SEM. The differences in tumor volume between LuCaP 86.2 treated with docetaxel 5 mgm weekly were highly significant ($P < 0.0001$) at the 8-week time period. There were no differences in LuCaP23.1 between vehicle or docetaxel treatment at any time point ($P > 0.05$). B, Western blot analysis for androgen receptor using α-ARN20 (top) and α-ARv7 in LuCaP 23.1, LuCaP 35, and LuCaP 86.2 showing the differences in the expression of androgen receptor and androgen receptor variants in the used xenografts. C, androgen receptor immunostaining in explanted LuCaP tumors showing the reduction in androgen receptor nuclear localization in LuCaP 86.2 xenograft. Top, representative pictures from untreated tumors (LuCaP 86.2, left side; LuCaP 23.1, right side); bottom, docetaxel (TXT)-treated tumors. D, percent of nuclear androgen receptor from explanted LuCaP tumors by androgen receptor immunostaining showing the statistically significant reduction of androgen receptor nuclear localization in LuCaP 86.2 xenograft when treated with docetaxel. ***, $P < 0.01$.

ARv567, and LuCaP 23.1, a human xenograft expressing both AR-wt and ARv7 (20). All xenografts were grown in noncastrate SCID mice. There were 15 mice in each group. As shown in Fig. 6A, LuCaP 86.2, which is resistant to castration and driven by ARv567, has its growth markedly suppressed by a low dose of docetaxel of 5 mg/kg ($P < 0.01$ control vs. docetaxel treated), a dose that we have previously shown to be ineffective on the growth of LuCaP 35 xenograft expressing primarily AR-wt (29). In contrast, there was no effect of docetaxel on the growth of LuCaP23.1 tumors (P = NS control vs. docetaxel treatment). The effect of docetaxel treatment on androgen receptor nuclear accumulation was further assessed by immunohistochemistry on explanted LuCaP tumors, as previously described (30). Quantitation of androgen receptor nuclear accumulation in tumors from untreated versus treated animals revealed that docetaxel treatment resulted in a statistically significant reduction of nuclear androgen receptor following in LuCaP86.2 tumors, whereas it had a minimal effect on LuCaP 23.1 tumors (Fig. 6B and C). These data support the hypothesis that drug-induced inhibition of androgen receptor nuclear accumulation underlies taxane antitumor activity and show that androgen receptor variant expression can determine taxane sensitivity *in vivo*.

Discussion

Prostate cancer, the most commonly diagnosed malignancy in males in the United States, depends on active androgen

Published OnlineFirst February 20, 2014; DOI: 10.1158/0008-5472.CAN-13-2876

receptor signaling (36). Androgen deprivation therapy alone is effective in a subset of patients with prostate cancer; however, many patients progress to CRPC. The discovery of androgen receptor splice variants has provided significant insight into mechanisms of disease progression and ADT resistance. However, the potential impact of androgen receptor splice variant expression on chemotherapy has not been investigated. Currently, the taxanes represent the standard of care in CRPC treatment. However, the therapeutic benefit of taxane treatment cannot be indefinitely sustained and currently we fail to understand the molecular basis of clinical taxane resistance. Herein, we provide evidence that the presence of androgen receptor splice variants may affect sensitivity to taxane treatment.

The clinical significance of these variants is highlighted by studies showing that elevated ARv7 expression is associated with more rapid disease recurrence following radical prostatectomy for localized disease (17, 18). In addition, it was recently shown that ARv7 is regulated by the transcriptional factor FOXO1 in a PTEN-PI3K-AKT dependent manner (37, 38), which is a pathway activated in 50% of prostate cancers.

The ARv567 variant, arising through skipping of exons 5 to 7 was identified in a panel of 25 different prostate cancer xenografts, termed the LuCaP series, most of which were derived from metastases obtained from men with CRPC after prolonged exposure to androgen-deprivation therapy (19). Unlike ARv7, ARv567 retains the hinge region that contains the second and most important part of androgen receptor's bipartite nuclear localization signal (NLS) consisting of aa ^{629}RKLKKL^{634} and responsible of AR/importin interaction (23, 26, 39). The hinge region contains also some well-defined control sites for androgen receptor activity, being target for acetylation, ubiquitylation, and methylation (23, 25).

However, even though androgen receptor variants have been found to increase the expression of full-length androgen receptor and enhance its transcriptional activity in the absence of ligand (19) their expression regulation and functional relationships had not been fully dissected. Studies on the transcriptional programs induced by variant signaling have shown that an adaptive shift toward androgen receptor–variant mediated signaling occurs in a subset of CRPC tumors, and thus suggesting that AR variants have different gene signatures from full-length androgen receptor potentially contributing to drug resistance to androgen receptor–targeted therapies such as abiraterone and enzalutamide (20, 21, 34). However, a recent report argues that androgen receptor variants induce genes that constitute a subset of the genes regulated by androgen receptor full length, rather than having a distinct transcriptional signature, and therefore, androgen receptor variants are constitutive and independent effectors of androgen receptor transcriptional program (21). Regardless of these discrepancies, the data on androgen receptor variants strongly suggest that their expression arises following castration and plays a role in the progression of prostate cancer.

For the variants to exert their transcriptional activity they have to be localized to the nucleus. Although the published literature highlights the strong nuclear presence of the variants, our results are the first to show a differential preference of androgen receptor variants for microtubule-mediated nuclear transport; ARv567 being microtubule- and dynein-dependent and ARv7 being microtubule independent (Figs. 4 and 5). Interestingly, we showed that the C-terminus of androgen receptor mediates microtubule binding (Fig. 1) and that the specific microtubule-binding domain comprises of the DNA-BD together with the adjacent hinge region (aa 559-663; Fig. 1C). This finding can readily explain the reduced association of ARv7 with microtubules, as ARv7 lacks the hinge region that mediates microtubule binding (Fig. 1C) and is also involved in the regulation of androgen receptor nuclear translocation and intranuclear motility (40). We were surprised to find that none of the individual C-terminus truncation mutants displayed as extensive microtubule association as the entire C-ter AR (aa 540-919; Fig. 2B and C). These results suggest that perhaps nonsequential regions of androgen receptor may come together in 3-dimension to generate the surface of microtubule interaction, indicating a larger and globular surface required for protein–protein interaction.

Additional studies using cryo-electron microscopy and recombinant full-length androgen receptor and androgen receptor variant proteins are currently ongoing in order to investigate the structural interaction between androgen receptor and its variants with microtubules. Our preliminary results have revealed that recombinant purified full-length androgen receptor protein binds directly to purified microtubules *in vitro* (data not shown), suggesting that androgen receptor may bind microtubules not only for the purpose of trafficking but also as a microtubule-associated protein potentially regulating polymer stability and dynamics.

We and others have previously shown that taxane treatment inhibits androgen receptor nuclear translocation and activity in prostate cancer cell lines and patient-derived CTCs (12, 13) and that this mechanism underlies at least in part clinical response to taxane treatment (14). While androgen receptor nuclear accumulation remains a critical factor responsible for androgen receptor transcriptional activity, the pathways regulating androgen receptor–variant nuclear translocation remain poorly understood. Our data support the requirement of the hinge region (aa 625-663) for androgen receptor microtubule association and downstream nuclear translocation, whereas other reports show that the NTD/DNA-BD core (aa 1-627) alone—in the absence of the hinge region—is sufficient for receptor nuclear translocation (28). At the same time mutation of 3 key residues of the hinge region, namely K630A, K632A, and K633A, completely abrogates nuclear accumulation of full-length androgen receptor in agreement with our results. These data suggest that in addition to microtubule-mediated androgen receptor nuclear transport, there are additional pathways that operate in the absence of the hinge region, like in the case of ARv7.

Clinically, although 50% of men respond to docetaxel following progression after standard androgen ablation, some men clearly are sensitive to taxanes and have a prolonged response, for reasons not well understood. In this report, we show that taxane-mediated microtubule stabilization differentially affects androgen receptor variant trafficking and transcriptional activity, raising the possibility that these variants

Published OnlineFirst February 20, 2014; DOI: 10.1158/0008-5472.CAN-13-2876

may predict sensitivity or resistance to taxane chemotherapy. In agreement with this hypothesis, we show that LuCaP human xenografts expressing ARv567 or full-length androgen receptor co-expressed with ARv7 show differential sensitivity to docetaxel treatment (Fig. 6). Interestingly, LuCaP 86.2 expressing predominantly ARv567 variant was the most sensitive to taxane treatment, consistent with the drug's ability to inhibit this variant's nuclear localization and activity. While our animal data do not indicate that androgen receptor inhibition is the only mechanism by which docetaxel is effective in prostate cancer, as we also showed that LuCaP xenografts that do not express high levels of ARv567 can respond to higher dose of docetaxel (Supplementary Fig. S4), LuCaP 86.2 is clearly an outlier in the sensitivity and duration of response to docetaxel.

Taken together, these data suggest that tumors driven by ARv567 may be marked as those that, even if resistant to next generation androgen receptor–targeting drugs, will likely benefit most by taxane treatment. Conversely, our data suggest that tumors predominantly expressing ARv7 will likely be resistant to taxane chemotherapy and that alternate treatments able to inhibit ARv7 transcriptional activity might be beneficial. Although the clinical impact of ARv7 expression on patient response to next generation androgen receptor–targeting drugs is not yet determined, our findings suggest that ARv7 expression may constitute a common mechanism of resistance to both taxanes and androgen receptor inhibitors. In agreement with this hypothesis, a recent clinical report showed that the activity of docetaxel in post- abiraterone–treated patients was lower than expected whereas no responses to docetaxel were observed in abiraterone-refractory patients (15). Moreover, a recent but not published clinical trial showed that men with hormone-sensitive metastatic prostate cancer who received docetaxel given at the start of ADT lived longer than patients who received hormone therapy alone (41). These recent findings are encouraging and strongly support the hypothesis that next-generation androgen receptor inhibitors and taxanes act on the same pathway (even if at a different level), and are synergistic in patients who presumably do not express significant amounts of androgen receptor variants because they are still responsive to ADT.

The data presented in this study provide insights into the regulation of androgen receptor–variant trafficking and activity in prostate cancer, link their expression with the therapeutic benefit of taxane treatment and suggest that the presence of androgen receptor variants may determine the clinical efficacy of taxane chemotherapy. Evaluating and discriminating androgen receptor variants in prostate cancer tumor cells can help clinicians tailor treatment in patient with CRPC by identifying patients who are most likely to benefit from taxane chemotherapy.

Disclosure of Potential Conflicts of Interest

D.M. Nanus is a consultant/advisory board member of Boehringer Ingelheim. P. Giannakakou has received a commercial research grant from Sanofi. No potential conflicts of interest were disclosed by the other authors.

Authors' Contributions

Conception and design: L. Portella, D.M. Nanus, P. Giannakakou
Development of methodology: L. Portella, M. Sung, A. Matov, P. Giannakakou
Acquisition of data (provided animals, acquired and managed patients, provided facilities, etc.): M. Thadani-Mulero, L. Portella, S. Sun, M. Sung, R.L. Vessella, E. Corey, S.R. Plymate
Analysis and interpretation of data (e.g., statistical analysis, biostatistics, computational analysis): M. Thadani-Mulero, L. Portella, A. Matov, R.L. Vessella, E. Corey, D.M. Nanus, S.R. Plymate, P. Giannakakou
Writing, review, and/or revision of the manuscript: M. Thadani-Mulero, L. Portella, A. Matov, D.M. Nanus, S.R. Plymate, P. Giannakakou
Administrative, technical, or material support (i.e., reporting or organizing data, constructing databases): S. Sun, M. Sung
Study supervision: P. Giannakakou

Grant Support

U.S. NIH (R01 CA137020-01 and U54 CA143876; P. Giannakakou), the NIH Physical Sciences Oncology Center at Cornell (P. Giannakakou and D.M. Nanus), NCI Pacific Northwest Prostate Cancer SPORE (2 P50 CA 097186-12; S.R. Plymate), PO1 CA85859 (S.R. Plymate), DOD-CDMRP (S.R. Plymate), the Prostate Cancer Foundation (S.R. Plymate), NCI PO1-163227-01A1 and DOD PC121152 (S.R. Plymate), the Prostate Cancer Foundation (R.L. Vessella), and the Department of Veterans Affairs Research Service (S.R. Plymate). Additional support was received from the Weill Cornell Clinical and Translational Science Center (D.M. Nanus and P. Giannakakou), the Prostate Cancer Foundation (P. Giannakakou and D.M. Nanus), the Italian Association for Cancer Research (AIRC) to L. Portella, NCI F32CA177104 to A. Matov, and the Genitourinary Oncology Research Fund (D.M. Nanus).

The costs of publication of this article were defrayed in part by the payment of page charges. This article must therefore be hereby marked *advertisement* in accordance with 18 U.S.C. Section 1734 solely to indicate this fact.

Received October 8, 2013; revised January 14, 2014; accepted January 30, 2014; published OnlineFirst February 20, 2014.

References

1. Hoffman-Censits J, Kelly WK. Enzalutamide: a novel antiandrogen for patients with castrate-resistant prostate cancer. Clin Cancer Res 2013;19:1335–9.
2. Tran C, Ouk S, Clegg NJ, Chen Y, Watson PA, Arora V, et al. Development of a second-generation antiandrogen for treatment of advanced prostate cancer. Science 2009;324:787–90.
3. de Bono JS, Logothetis CJ, Molina A, Fizazi K, North S, Chu L, et al. Abiraterone and increased survival in metastatic prostate cancer. N Engl J Med 2011;364:1995–2005.
4. Nelson PS. Molecular states underlying androgen receptor activation: a framework for therapeutics targeting androgen signaling in prostate cancer. J Clin Oncol 2012;30:644–6.
5. Locke JA, Guns ES, Lubik AA, Adomat HH, Hendy SC, Wood CA, et al. Androgen levels increase by intratumoral *de novo* steroidogenesis during progression of castration-resistant prostate cancer. Cancer Res 2008;68:6407–15.
6. Chen CD, Welsbie DS, Tran C, Baek SH, Chen R, Vessella R, et al. Molecular determinants of resistance to antiandrogen therapy. Nat Med 2004;10:33–9.
7. Nadiminty N, Gao AC. Mechanisms of persistent activation of the androgen receptor in CRPC: recent advances and future perspectives. World J Urol 2012;30:287–95.
8. Joseph JD, Lu N, Qian J, Sensintaffar J, Shao G, Brigham D, et al. A clinically relevant androgen receptor mutation confers resistance to second-generation antiandrogens enzalutamide and ARN-509. Cancer Discov 2013;3:1020–9.
9. Korpal M, Korn JM, Gao X, Rakiec DP, Ruddy DA, Doshi S, et al. An F876L mutation in androgen receptor confers genetic and phenotypic

Published OnlineFirst February 20, 2014; DOI: 10.1158/0008-5472.CAN-13-2876

resistance to MDV3100 (Enzalutamide). Cancer Discov 2013;3:1030–43.
10. Petrylak DP, Tangen CM, Hussain MH, Lara PN Jr., Jones JA, Taplin ME, et al. Docetaxel and estramustine compared with mitoxantrone and prednisone for advanced refractory prostate cancer. N Engl J Med 2004;351:1513–20.
11. Tannock IF, de Wit R, Berry WR, Horti J, Pluzanska A, Chi KN, et al. Docetaxel plus prednisone or mitoxantrone plus prednisone for advanced prostate cancer. N Engl J Med 2004;351:1502–12.
12. Darshan MS, Loftus MS, Thadani-Mulero M, Levy BP, Escuin D, Zhou XK, et al. Taxane-induced blockade to nuclear accumulation of the androgen receptor predicts clinical responses in metastatic prostate cancer. Cancer Res 2011;71:6019–29.
13. Zhu ML, Horbinski CM, Garzotto M, Qian DZ, Beer TM, Kyprianou N. Tubulin-targeting chemotherapy impairs androgen receptor activity in prostate cancer. Cancer Res 2010;70:7992–8002.
14. Thadani-Mulero M, Nanus DM, Giannakakou P. Androgen receptor on the move: boarding the microtubule expressway to the nucleus. Cancer Res 2012;72:4611–5.
15. Mezynski J, Pezaro C, Bianchini D, Zivi A, Sandhu S, Thompson E, et al. Antitumour activity of docetaxel following treatment with the CYP17A1 inhibitor abiraterone: clinical evidence for cross-resistance? Ann Oncol 2012;23:2943–7.
16. Dehm SM, Schmidt LJ, Heemers HV, Vessella RL, Tindall DJ. Splicing of a novel androgen receptor exon generates a constitutively active androgen receptor that mediates prostate cancer therapy resistance. Cancer Res 2008;68:5469–77.
17. Guo Z, Yang X, Sun F, Jiang R, Linn DE, Chen H, et al. A novel androgen receptor splice variant is up-regulated during prostate cancer progression and promotes androgen depletion-resistant growth. Cancer Res 2009;69:2305–13.
18. Hu R, Dunn TA, Wei S, Isharwal S, Veltri RW, Humphreys E, et al. Ligand-independent androgen receptor variants derived from splicing of cryptic exons signify hormone-refractory prostate cancer. Cancer Res 2009;69:16–22.
19. Sun S, Sprenger CC, Vessella RL, Haugk K, Soriano K, Mostaghel EA, et al. Castration resistance in human prostate cancer is conferred by a frequently occurring androgen receptor splice variant. J Clin Invest 2010;120:2715–30.
20. Mostaghel EA, Marck BT, Plymate SR, Vessella RL, Balk S, Matsumoto AM, et al. Resistance to CYP17A1 inhibition with abiraterone in castration-resistant prostate cancer: induction of steroidogenesis and androgen receptor splice variants. Clin Cancer Res 2011;17:5913–25.
21. Li Y, Chan SC, Brand LJ, Hwang TH, Silverstein KA, Dehm SM. Androgen receptor splice variants mediate enzalutamide resistance in castration-resistant prostate cancer cell lines. Cancer Res 2013;73:483–9.
22. Hornberg E, Ylitalo EB, Crnalic S, Antti H, Stattin P, Widmark A, et al. Expression of androgen receptor splice variants in prostate cancer bone metastases is associated with castration-resistance and short survival. PLoS ONE 2011;6:e19059.
23. Clinckemalie L, Vanderschueren D, Boonen S, Claessens F. The hinge region in androgen receptor control. Mol Cell Endocrinol 2012;358:1–8.
24. Cutress ML, Whitaker HC, Mills IG, Stewart M, Neal DE. Structural basis for the nuclear import of the human androgen receptor. J Cell Sci 2008;121:957–68.
25. Haelens A, Tanner T, Denayer S, Callewaert L, Claessens F. The hinge region regulates DNA binding, nuclear translocation, and transactivation of the androgen receptor. Cancer Res 2007;67:4514–23.
26. Zhou ZX, Sar M, Simental JA, Lane MV, Wilson EM. A ligand-dependent bipartite nuclear targeting signal in the human androgen receptor. Requirement for the DNA-binding domain and modulation by NH2-terminal and carboxyl-terminal sequences. J Biol Chem 1994;269:13115–23.
27. Giannakakou P, Sackett DL, Ward Y, Webster KR, Blagosklonny MV, Fojo T. p53 is associated with cellular microtubules and is transported to the nucleus by dynein. Nat Cell Biol 2000;2:709–17.
28. Chan SC, Li Y, Dehm SM. Androgen receptor splice variants activate androgen receptor target genes and support aberrant prostate cancer cell growth independent of canonical androgen receptor nuclear localization signal. J Biol Chem 2012;287:19736–49.
29. Wu JD, Haugk K, Coleman I, Woodke L, Vessella R, Nelson P, et al. Combined *in vivo* effect of A12, a type 1 insulin-like growth factor receptor antibody, and docetaxel against prostate cancer tumors. Clin Cancer Res 2006;12:6153–60.
30. Zhang X, Morrissey C, Sun S, Ketchandji M, Nelson PS, True LD, et al. Androgen receptor variants occur frequently in castration resistant prostate cancer metastases. PLoS ONE 2011;6:e27970.
31. Rosin P. Unimodal thresholding. Pattern Recognit 2001;34:2083–96.
32. Aurenhammer F, Klein R. Voronoi Diagrams. Handbook of computational geometry. Amsterdam: North-Holland; 2000. p. 201–90.
33. Watson PA, Chen YF, Balbas MD, Wongvipat J, Socci ND, Viale A, et al. Constitutively active androgen receptor splice variants expressed in castration-resistant prostate cancer require full-length androgen receptor. Proc Natl Acad Sci U S A 2010;107:16759–65.
34. Hu R, Lu C, Mostaghel EA, Yegnasubramanian S, Gurel M, Tannahill C, et al. Distinct transcriptional programs mediated by the ligand-dependent full-length androgen receptor and its splice variants in castration-resistant prostate cancer. Cancer Res 2012;72:3457–62.
35. Burkhardt JK, Echeverri CJ, Nilsson T, Vallee RB. Overexpression of the dynamitin (p50) subunit of the dynactin complex disrupts dynein-dependent maintenance of membrane organelle distribution. J Cell Biol 1997;139:469–84.
36. Sharma NL, Massie CE, Ramos-Montoya A, Zecchini V, Scott HE, Lamb AD, et al. The androgen receptor induces a distinct transcriptional program in castration-resistant prostate cancer in man. Cancer Cell 2013;23:35–47.
37. Bohrer LR, Liu P, Zhong J, Pan Y, Angstman J, Brand LJ, et al. FOXO1 binds to the TAU5 motif and inhibits constitutively active androgen receptor splice variants. Prostate 2013;73:1017–27.
38. Mediwala SN, Sun H, Szafran AT, Hartig SM, Sonpavde G, Hayes TG, et al. The activity of the androgen receptor variant AR-V7 is regulated by FOXO1 in a PTEN-PI3K-AKT-dependent way. Prostate 2013;73:267–77.
39. Claessens F, Denayer S, Van Tilborgh N, Kerkhofs S, Helsen C, Haelens A. Diverse roles of androgen receptor (AR) domains in AR-mediated signaling. Nucl Recept Signal 2008;6:e008.
40. Tanner TM, Denayer S, Geverts B, Van Tilborgh N, Kerkhofs S, Helsen C, et al. A 629RKLKK633 motif in the hinge region controls the androgen receptor at multiple levels. Cell Mol Life Sci 2010;67:1919–27.
41. Sweeney C. NIH-funded study shows increased survival in men with metastatic prostate cancer who receive chemotherapy when starting hormone therapy; 2013 [cited 2013 Dec 5]. Available from: http://www.cancer.gov/newscenter/newsfromnci/2013/E3805.

Cancer Research
The Journal of Cancer Research (1916–1930) | The American Journal of Cancer (1931–1940)

AACR American Association for Cancer Research

Androgen Receptor Splice Variants Determine Taxane Sensitivity in Prostate Cancer

Maria Thadani-Mulero, Luigi Portella, Shihua Sun, et al.

Cancer Res 2014;74:2270-2282. Published OnlineFirst February 20, 2014.